PAPER

Synthesis of mono-, di-, and triaminobismuthanes and observation of C−C coupling of aromatic systems with bismuth(III) chloride†

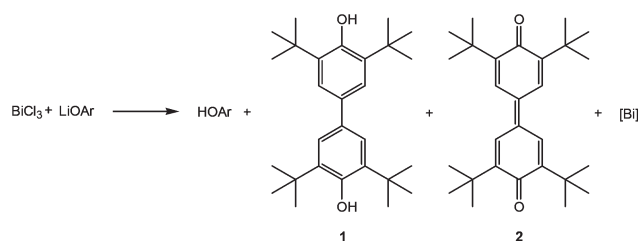Christian Hering-Junghans,[a,b] Axel Schulz,*[a,c] Max Thomas[a] and Alexander Villinger[a]

The reaction of lithium *N*-trimethylsilyl-amides of the type RN(SiMe₃)Li with bismuth(III) chloride yielded mono-, di- or triaminobismuthanes depending on the steric demand of the anilide ligand R and the used stoichiometry. For the bulky Mes* substituent the reaction with BiCl₃ resulted in the formation of a C−C coupling product as the main product besides a small amount of the expected Mes*N(SiMe₃)BiCl₂.
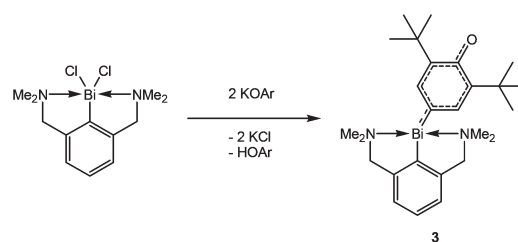
Introduction

C–C coupling reactions of aromatic systems in the presence of bismuth(III) chloride have been known since 2002, when Hanna and coworkers described the reaction of LiOAr (Ar = 2,6-di-*tert*-butylphenyl) with BiCl₃.[1] A complex mixture of organic compounds along with a black precipitate was observed by the authors. Beside HOAr, the main products of this reaction were a diol (**1**) and a dione (**2**) as illustrated in Scheme 1,[1,2] and their formation can be rationalized by a mechanism involving radical intermediates.

With the aid of EPR spectroscopy Hanna and coworkers could experimentally detect Bi(II) radicals in the reaction mixture.[1] In 2011 the group of Evans reported the preparation of a formal Bi(II) species with an NCN pincer-type ligand and a CH-activated ArO-group (Ar = 2,6-ditertbutylphenyl) binding to bismuth through the 4-position (**3**, Scheme 2).[2] In contrast the reaction of the BiCl₂-precursor with KOAr′ (Ar′ = Dmp, 2,6-dimethylphenyl; Dipp, 2,6-diisopropylphenyl) substituents yielded the corresponding oxidobismuthanes, a C–H activation of the *para*-position could not be observed. In 2014, Evans *et al.* presented a catalytic cycle based on their pincer complex **3** (Scheme 2).[3]

With this complex in hand, the group of Evans was able to introduce a carboxyl group using 2,6-di-*tert*-butylphenolat and

Scheme 1 Reaction of LiOAr with BiCl₃ by Hanna *et al.* (Ar = 2,6-di-*tert*-butylphenyl).

Scheme 2 Synthesis of **3** by Evans *et al.* (Ar = 2,6-di-*tert*-butylphenyl).

CO₂ as starting materials. The carboxyl group in this reaction could also be replaced by a NO functionality.[4] Just recently, a stable Bi(II)-radical was reported by the Coles group, making this a vital field of research.[5] To the best of our knowledge, there are no similar reactions of amides (**4**, R = aryl in Scheme 3) reported. Herein, we report on the systematic study of silylated bulky mono-, di- and triaminobismuthanes of the type RN(SiMe₃)BiCl₂, [RN(SiMe₃)]₂BiCl and [RN(SiMe₃)]₃Bi. There is only scarce information on substituted aminobismuthanes[6] which are valuable starting materials for several transformations in main group chemistry such as the
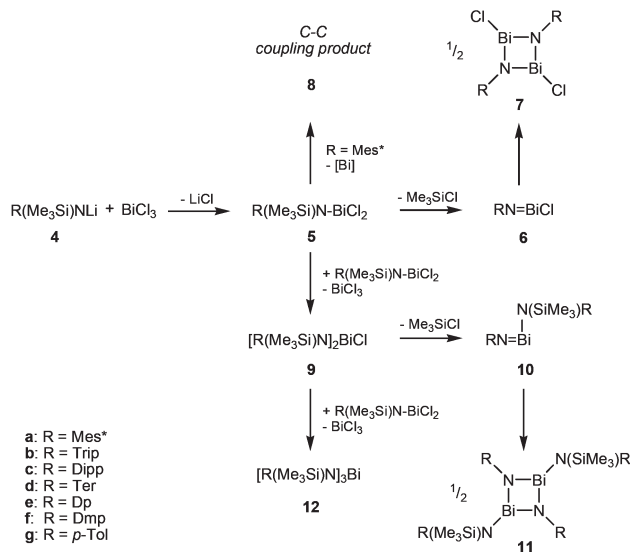
[a]Institut für Chemie, Universität Rostock, Albert-Einstein-Str. 3a, 18059 Rostock, Germany. E-mail: axel.schulz@uni-rostock.de
[b]Department of Chemistry, University of Alberta, 11227 Saskatchewan Dr., T62 2G2 Edmonton, Alberta, Canada
[c]Abteilung Materialdesign, Leibniz-Institut für Katalyse e.V. an der Universität Rostock, Albert-Einstein-Str. 29a, 18059 Rostock, Germany
†Electronic supplementary information (ESI) available: Additional experimental details, full characterization of all compounds. CCDC 1447892–1447910. For ESI and crystallographic data in CIF or other electronic format see DOI: 10.1039/c6dt00229c

Scheme 3 Product distribution in the synthesis of mono-, di- and tri-amino bismuthanes.

generation of *cyclo*-dibismadiazanes $[R'Bi(\mu\text{-}NR)]_2$,[7–9] bismuthenium cations,[10–14] or Bi–N precursors.[15–23] For example, $Bi(NMe_2)_3$ is used in CVD (chemical vapour deposition) processes to deposit bismuth nitrides as suggested by Errington and Norman.[23] The isolation of (silylated) aminobismuthanes is complicated since often coincident formation of monoamino-dichloro-, diaminochloro-, and triaminobismuthanes can be observed (Scheme 3). Additionally, Me_3SiCl-elimination can result in the formation of iminobismuthanes or their respective dimers, the dibismadiazanes, can be obtained depending on the bulkiness of the substituents.[24] Hence, it is vital to find specific synthetic protocols to generate specific aminobismuthanes, iminobismuthanes or *cyclo*-dibismadiazane, exclusively. This can be achieved by the utilization of Me_3Si-substituted bulky amido groups $N(SiMe_3)R$ (Scheme 3) and by the use of lithium amides rather than amines.
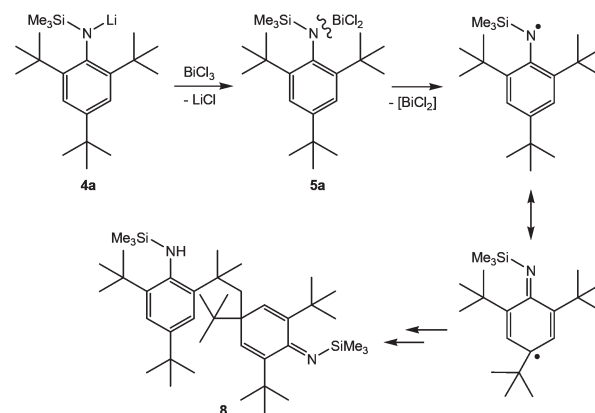
Results and discussion

Syntheses

In a series of experiments we studied the reaction of $BiCl_3$ with 1, 2 and 3 equivalents of $Li[N(SiMe_3)R]$ (R = Mes* (**4a**), Trip (**4b**), Dipp (**4c**), Ter (**4d**), Dp (**4e**), Dmp (**4f**), *p*-Tol (**4g**); Mes* = 2,4,6-tri-*tert*-butylphenyl, Trip = 2,4,6-triisopropylphenyl, Dipp = 2,6-diisopropylphenyl, Ter = 2,6-bis(2,4,6-trimethylphenyl)-phenyl, Dp = 3,4-dimethylphenyl, Dmp = 2,6-dimethylphenyl, *p*-Tol = 4-methylphenyl) at ambient temperature. The lithium amides **4** were readily obtained in the reaction of the respective *N*-trimethylsilyl-aniline derivatives with *n*-BuLi, whereas in most cases **4** can be generated *in situ* prior to the reaction with $BiCl_3$.

Astonishingly, treatment of $BiCl_3$ with equimolar amounts of **4** resulted, depending on the steric strain, in a complex mixture of products as illustrated in Scheme 3 (*cf.* steric strain can be evaluated using the maximal cone angle at 1.45 Å:[25] 251° Mes*, 222° Trip, 223° Dipp, 232° Ter, 158° Dp, 199° Dmp, 158° *p*-Tol).

Reaction with 4a. Surprisingly, the reaction of $Mes*N(SiMe_3)Li$ (**4a**), which was usually formed *in situ* from $Mes*N(SiMe_3)H$ and *n*-BuLi, with one equivalent of $BiCl_3$ in thf at ambient temperature led to C–C coupling product **8** besides a black precipitation of bismuth and bismuth chlorides as depicted in Schemes 3 and 4. In analogy to the observation of Hanna and co-workers, a radical mechanism is also assumed in this case.

Upon addition of a solution of $Mes*N(SiMe_3)Li$ at room temperature to a suspension of $BiCl_3$ first the formation of $Mes*N(SiMe_3)BiCl_2$ (**5a**) was observed as indicated by ^1H NMR data. The yellow solution darkens upon complete addition of **4a** and eventually gave the aforementioned black suspension. Presumably, decomposition is initiated by homolytic dissociation of the N–Bi bond affording, after a complex rearrangement, C–C coupling product **8** besides a black mixture of bismuth containing compounds (for example $BiCl_3$ thf could be identified) as illustrated in Scheme 4. It needs to be emphasized that the formation of **8** under this reaction conditions is reproducible and usually yields **8** in isolated yields of 40–50% with respect to **4a** (Fig. 1). When the addition of **4a** to $BiCl_3$ was carried out at low temperatures (−80 °C), we were successful to isolate **5a** in small amounts besides **8** (1 : 9 ratio) upon slow warming to −20 °C and fractional crystallization. Hence, this experimentally proves that the initial formation of **5a** represents the first reaction step as discussed before. The presence of **5a** was unequivocally confirmed by X-ray diffraction (Fig. 2). Crystals of **5a** 1.5 toluene were obtained from recrystallization in toluene (Fig. 2). Using isolated and recrystallized **4a** rather than generating it *in situ* (in the reaction with $BiCl_3$ in diethyl ether at −80 °C) suppressed the formation of the C–C coupling product, however, not entirely. It was possible to obtain **5a** as the main product in using this protocol. Using freshly sublimed $BiCl_3$ also helped to increase the

Scheme 4 Formation of **5a** and postulated reaction to the coupling product **8** in analogy to the suggested reaction pathway by Hanna *et al.*
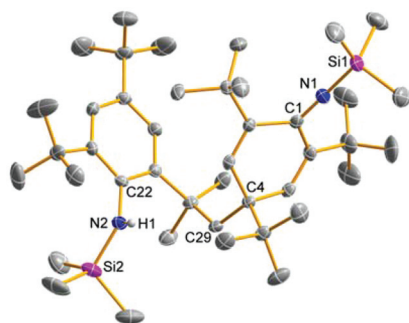
Fig. 1 ORTEP drawing of the molecular structure of **8**. Thermal ellipsoids with 50% probability at 173 K (hydrogen atoms omitted for clarity except from N–H). Selected distances (Å) and angles (°): Si1–N1 1.689(2), Si2–N2 1.732(2), N1–C1 1.268(2), N2–C22 1.438(2), C29–C4 1.565(3), Si1–N1–C1 175.9(2), N2–Si2–C22 135.2(2).
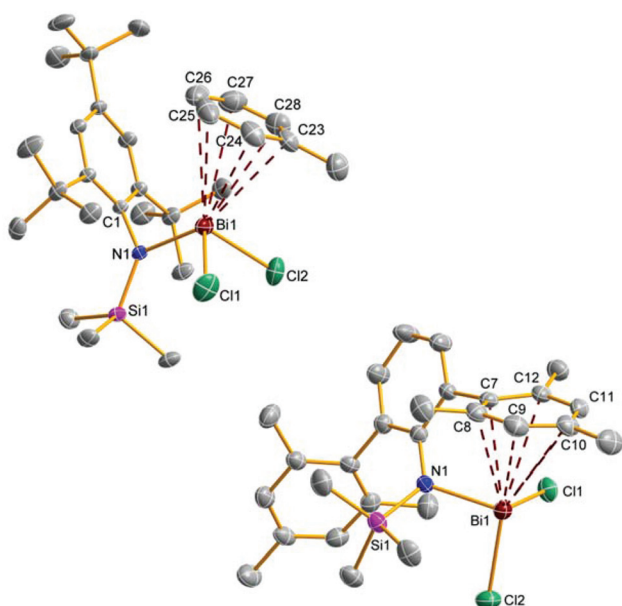

Fig. 2 ORTEP drawing of the molecular structure of **5a** (left) and **5d** (right). Thermal ellipsoids with 50% probability at 173 K (hydrogen atoms omitted for clarity). Selected distances (Å) and angles (°): **5a**: Bi1–N1 2.146(1), Bi1–Cl1 2.4771(5), Bi1–Cl2 2.4920(5), N1–Si1 1.747(2), Bi1–C23 3.340(2), Bi1–C24 3.376(2), Bi1–C25 3.474(3), Bi1–C26 3.517(2), Bi1–C27 3.472(3), Bi1–C28 3.386(3), Cl1–Bi1–Cl2 89.86(2), Cl2–Bi1–N1 103.57(3), N1–Bi1–Cl1 99.82(3), Bi1–N1–C1 101.49(8); **5d**: Bi1–N1 2.176(3), Bi1–Cl1 2.485(1), Bi1–Cl2 2.517(1), Bi1–C7 2.940(4), Bi1–C8 3.223(4), Bi1–C9 3.524(5), Bi1–C10 3.637(4), Bi1–C11 3.484(4), Bi1–C12 3.191(4), N1–Bi1–Cl1 100.31(8), N1–Bi1–Cl2 94.09(8), Cl1–Bi1–Cl2 87.64(3), Bi1–N1–C1 118.3(2).

amount of **5a** formed and suppressed formation of **8**. The influence of freshly sublimed $BiCl_3$ was already discussed by Evans *et al.* in the synthesis of $Bi[N(SiM_3)_2]_3$.[26] In the reaction with **4a** the as supplied bismuth(III)-chloride tends to pronounce the formation of **8**. **5a** is stable in the solid state with respect to the formation of **8**. In dichloromethane solution the formation of a black precipitate indicated a partial decompo-

sition within 120 h at room temperature, but no decomposition products could be identified in the ^{1}H NMR spectrum, which suggest decomposition into NMR-silent or insoluble products. Interestingly, Burford and co-workers reported the formation of $(Mes*NH)_3Bi$ in the reaction of three equivalents of the corresponding lithium amide with one equivalent $BiCl_3$.[27] Obviously, substitution of H by Me_3Si prevents a higher degree of substitution at the bismuth.

We were interested in the generality of this C–C coupling reaction, prompting us to study differently substituted *N*-trimethylsilyl-amides, however, C–C coupling processes were only observed for the very bulky Mes* substituent.

Reaction with 4b. Treatment of **4b** with $BiCl_3$ in thf or diethyl ether resulted in the formation of the bis-substituted product $[TripN(SiMe_3)]_2BiCl$ (**9b**, Fig. 4). The mono-substituted product **5b** (Fig. 3) was only formed as a byproduct in minor quantities and could not be fully characterized. Recrystallization of the crude material from *n*-hexane gave single crystals of **9b** in moderate yield (55%). Moreover, formation of $TripN-(SiMe_3)H$ was detected by ^{1}H NMR spectroscopy. In contrast to **5a** no C–C coupling reaction was observed. **5b** was only observed as a by-product besides **9b**, therefore **5b** could not be fully characterized. Due to the bulky Trip substituent, the threefold substitution product **12b** was not observed. Utilizing two or three equivalents of **4b**, $TripN(SiMe_3)H$ was observed as main product by ^{1}H NMR spectroscopy.

Reaction with 4c. The Dipp substituted aniline **4c** $Li[N(SiMe_3)Dipp]$ showed nearly the same reactivity in the

Fig. 3 ORTEP drawing of the molecular structure of **5b** (top, only one independent molecule is shown) and representation of the chain-like structure in the crystal of **5b** (bottom, view along *b*-axis). Thermal ellipsoids with 50% probability at 173 K (hydrogen atoms omitted for clarity). Selected distances (Å) and angles (°): Bi1–Cl1 2.449(1), Bi1–Cl2 2.482(1), Bi1–Cl3 2.4946(9), Bi2–Cl4 2.5063(9), Bi1–N1 2.111(3), Bi2–N2 2.133(3), N1–Bi1–Cl1 97.84(7), Cl1–Bi1–Cl2 93.85(4), Cl2–Bi1–N1 97.05(7); long range distances: Bi2'–Cl4 3.593(1), Bi2'–Cl2' 3.359(1), Bi1'–Cl3' 3.755(1), Bi1–Cl3' 3.761(1).

reaction with $BiCl_3$ compared to **4b**. With a short reaction time and immediate work-up the 1 : 1 stoichiometry resulted in the formation of mono-substitution product $DippN(SiMe_3)BiCl_2$ (**5c**), which could be crystalized beside $[DippN(SiMe_3)]_2BiCl$ (**9c**). Unfortunately, even isolated crystals of **5c** were contaminated with **9c** and thus could not be fully characterized. Interestingly, reaction of two or three equivalents **4c** with bismuth(III)-chloride afforded $DippN(SiMe_3)H$ as the main product. In analogy to this reaction Roesky and co-workers demonstrated that the reaction of two or three equivalents of $DippN(H)Li$ with $BiCl_3$ led to a four-membered heterocycle of the type $[DippNBiN(H)Dipp]_2$, the dimerization product of the intermediately formed iminobismuthane, similar to ring **11** (Scheme 3).[28] Burford *et al.* reported a similar reaction but added t-BuN(H)Li as additional base to the reaction mixture of $DippN(H)Li$ and $BiCl_3$. This reaction also afforded $[DippNBiN-(H)Dipp]_2$ but in higher yields and with an easier isolation of the four-membered ring system, because the byproduct t-BuNH$_2$ is considerably easier to remove than $DippNH_2$.[24]

Reaction with 4d. Since the terphenyl substituent is rather bulky, neither C–C coupling nor multi-substitution products (**9d**, **12d**) could be detected. Only the mono-substitution product $TerN(SiMe_3)BiCl_2$ (**5d**) was afforded and isolated in rather low yields (*ca.* 35%). Re-crystallization from CH_2Cl_2 gave single crystals suitable for X-ray structure elucidation (Fig. 2, left). In case of the reaction of two or three equivalents of the lithium amide, again the formation of $TerN(SiMe_3)H$ was observed.

Reaction with 4e. When $BiCl_3$ was treated with only one equivalent of $Li[N(SiMe_3)Dp]$ **4e** a mixture of $DpN(SiMe_3)BiCl_2$ (**5e**) and $[DpN(SiMe_3)]_2BiCl$ (**9e**) (Scheme 3) was detected in thf solution from which single-crystals (**5e/9e**) of a 1 : 1 mixture of **5e** and **9e** were obtained (Fig. 5). Generally, both the double as well as the triple substitution product can either be formed by reaction of **5e** with **4e** and **9e** with **4e**, respectively, or as depicted in Scheme 3 by $BiCl_3$ elimination from **5e** and **9e** respectively. As shown in Fig. 5, in the solid state structure of **5e/9e** $BiCl_3$ moieties are preformed, so it can be assumed that in solution dimeric or even oligomeric units are present which react under $BiCl_3$ elimination to give the triaminobismuthane **12e**. Crystals of **5e/9e** are only stable in the solid state, in solution they readily release $BiCl_3$ affording **12e** (Fig. 6), which is also the main product, when three equivalents of **4e** are reacted with $BiCl_3$.

Reaction with 4f. Treatment of $BiCl_3$ with one equivalent of **4f** always resulted in the formation of mixtures of products which could not be effectively separated (Scheme 3). When two or three equivalents of the amide **4f** were added to a suspension of unsublimed $BiCl_3$, amino-substituted four-membered ring **11f** was formed (Fig. 7) besides unreacted **4f** and could be isolated by crystal picking. In an analogous reaction using three equivalents of $KN(SiMe_3)_2$ and one equivalent of as received $BiCl_3$, Evans *et al.* reported the formation of a *cyclo*-dibismadiazane similar to the structure of **11** with R = Me$_3$Si *via* formal loss of a SiMe$_3$ group, while the use of freshly sublimed $BiCl_3$ yielded $Bi[N(SiMe_3)_2]_3$ in high yields.[26] If freshly

sublimed $BiCl_3$ was reacted with three equivalents of **4f** a mixture of products was formed from which no substance could be isolated.

Reaction with 4g. The reaction of $Li[N(SiMe_3)p$-Tol] **4g** with $BiCl_3$ in a 1 : 1 stoichiometry led to a mixture of products. From this mixture we were able to isolate the triple substitution product $[p$-TolN(SiMe_3)]_3Bi$ (**12g**) as pale yellow crystals suitable for X-ray structure elucidation (Fig. 6). However, utilization of an excess of base **4g** (2 or 3 equivalents) resulted in

Table 1 Selected structural data of all isolated single-crystalline solids (*d* in Å, < in °)

	Bi–Cl	Bi–N	Cl–Bi–Cl	Cl–Bi–N	N–Bi–N
5a	2.4771(5)	2.146(1)	89.9(2)	99.82(3)	—
	2.4920(5)	—	—	103.57(3)	—
5b	2.449(1)	2.111(3)	93.85(4)	97.05(7)	—
	2.483(1)	—	—	97.84(7)	—
9b	2.4862(7)	2.140(2)	—	95.83(5)	108.51(7)
	—	2.178(2)	—	97.35(5)	—
5c	2.4746(9)	2.125(3)	94.90(3)	92.50(7)	—
	2.5124(9)	—	—	95.99(7)	—
	2.4687(8)	2.128(2)	84.24(3)	101.95(7)	—
	2.6409(8)	—	—	94.48(7)	—
	2.4631(8)	2.142(2)	92.16(3)	93.19(7)	—
	2.6580(8)	—	—	96.16(7)	—
	2.4369(9)	2.126(3)	97.86(3)	95.89(8)	—
	2.515(1)	—	—	94.58(7)	—
9c	2.497(2)	2.170(3)	—	96.48(9)	112.5(2)
	—	2.147(3)	—	98.6(1)	—
	2.477(1)	2.182(3)	—	95.17(8)	110.7(1)
	—	2.148(3)	—	96.74(8)	—
5d	2.485(1)	2.176(3)	87.64(3)	94.09(8)	—
	2.517(1)	—	—	100.31(8)	—
5e in **5e/9e**	2.550(2)	2.116(6)	89.60(7)	94.7(1)	—
	2.470(2)	—	—	95.2(2)	—
9e in **5e/9e**	2.581(2)	2.137(6)	—	94.6(2)	95.7(2)
	—	2.141(6)	—	97.9(2)	—
12e	—	2.159(3)	—	—	98.7(1)
	—	2.155(3)	—	—	97.9(1)
	—	2.155(3)	—	—	98.5(1)
11f[c]	—	2.176(9)[a]	—	—	99.5(3)[b]
	—	2.175(9)[a]	—	—	102.1(3)[b]
	—	2.16(1)	—	—	98.7(3)[b]
	—	2.142(7)	—	—	101.7(3)[b]
	—	2.154(9)	—	—	77.1(3)
	—	2.164(7)	—	—	77.7(3)
11g[d]	—	2.165(2)[a]	—	—	96.61(8)[b]
	—	2.129(2)	—	—	75.62(8)
	—	2.147(2)	—	—	95.29(8)
12g	—	2.150(3)	—	—	98.5(1)
	—	2.162(3)	—	—	98.6(1)
	—	2.154(3)	—	—	98.0(1)

[a] Exocyclic Bi–N distance. [b] N$_{ring}$–Bi–N$_{exocyclic}$. [c] Ring adopts C_1 symmetry. [d] Ring adopts C_i symmetry.

the formation of **12g** (80%) when freshly sublimed BiCl$_3$ was added. Interestingly, when BiCl$_3$ was used as delivered by Alfa Aesar traces of four-membered heterocycle **11g** were observed. Red crystals of **11g** suitable for X-ray structure determination were isolated from such an experiment.

X-ray elucidation

X-ray quality crystals were selected in Fomblin YR-1800 perfluoroether (Alfa Aesar) at ambient temperature. The samples were cooled to 173(2) K during measurement. Selected structural data are listed in Table 1, the molecular structures are shown in Fig. 1–7.

As expected the molecular structures of all bismuth species feature a strongly distorted trigonal pyramidal coordination environment about the Bi center. Despite the pyramidal Bi centers, the four-membered rings in **11g** and **11f** are planar with both exocyclic amino groups in a *trans* orientation (deviation from planarity **11f**: 0.0°, **11g**: <2°). As can be seen from the data in Table 1, the molecular structures of all considered species display a fairly sharp distribution of Bi–N distances between 2.111–2.182 Å in accord with a typical polar Bi–N single bond (cf. $\sum r_{cov}$(Bi–N) = 2.22 Å;[29] 2.16–2.17 Å in [DipNBiN(H)Dip]$_2$]).[24,28]

The Bi–Cl bond lengths are in the range between 2.4369 to 2.658 Å, which is also indicative single bonds ($\sum r_{cov}$(Bi–Cl) = 2.50 Å).[29] With respect to the angles around the bismuth center, the following trend was observed: <(Cl–Bi–Cl) (84.2–97.9°) ≪ (Cl–Bi–N) (92.5–103.6°) ≪ (N–Bi–N) (95.7–112.5°) which can mainly be attributed to the bulky Me$_3$Si and phenyl substituents attached to the N atoms.

The most prominent structural features are secondary inter- and intramolecular interactions stabilizing the Lewis acidic bismuth center. Three different types of such interactions were observed: (i) intramolecular π-arene⋯Bi contacts, (ii) intermolecular π-arene⋯Bi contacts and (iii) chlorine atoms as bridges between different Bi centers. Strong secondary interactions of type (i) (Menshutkin type π complexes)[30] with one phenyl group of the terphenyl substituent were observed for **5d** (Fig. 2) as indicated by very short Bi⋯C$_{arene}$ distances
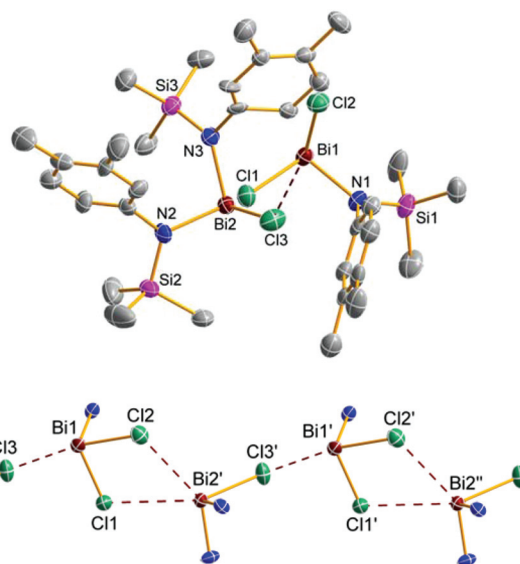

Fig. 5 ORTEP drawing of the molecular structure of **5e/9e** (top) and representation of the chain-like structure in the crystal of **5e/9e** (bottom, view along *a*-axis). Thermal ellipsoids with 50% probability at 173 K (hydrogen atoms omitted for clarity). Selected distances (Å) and angles (°): Bi1–Cl1 2.4702(2), Bi1–Cl2 2.550(2), Bi2–Cl3 2.581(2), Bi1–N1 2.116(6), Cl2–Bi1–Cl3 171.000(6), Cl1–Bi1–Cl3 83.360(7); long range distances: Bi1–Cl3 3.057(2), Bi2′–Cl1 3.516(2), Bi2′–Cl2 3.644(2), Bi1–Bi2 4.8481(3).
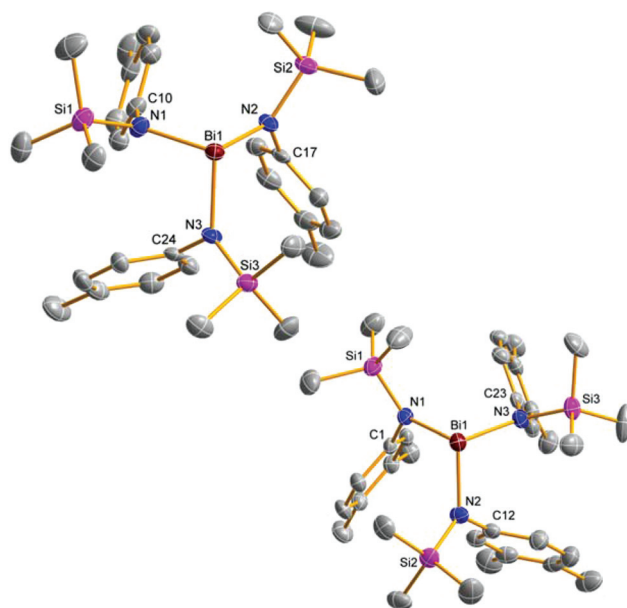

Fig. 6 ORTEP drawing of the molecular structure of **12g** (top) and **12e** (bottom). Thermal ellipsoids with 50% probability at 173 K (hydrogen atoms omitted for clarity). Selected distances (Å) and angles (°): **12g**: Bi1–N1 2.150(3), Bi1–N2 2.162(3), Bi1–N3 2.154(3), N1–Bi1–N2 98.6(1), N2–Bi1–N3 98.6(1), N3–Bi1–N1 98.0(1); **12e**: Bi1–N1 2.159(3), Bi1–N2 2.155(3), Bi1–N3 2.155(3), N1–Bi1–N2 98.5(1), N2–Bi1–N3 97.9(1), N3–Bi1–N1 98.7(1).

Fig. 4 ORTEP drawing of the molecular structure of **9b**. Thermal ellipsoids with 50% probability at 173 K (hydrogen atoms omitted for clarity). Selected distances (Å) and angles (°): Bi1–Cl1 2.4862(7), Bi1–N1 2.140(2), Bi1–N2 2.179(2), N1–Bi1–Cl1 97.35(5), Cl1–Bi1–N2 95.83(5), N2–Bi1–N1 108.50(7).
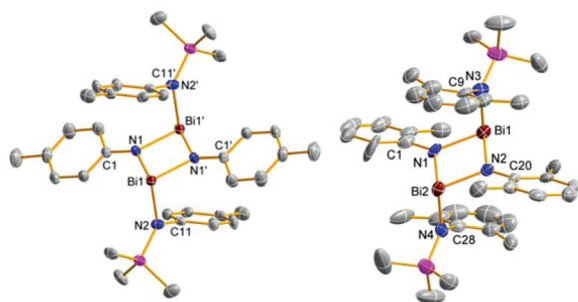
Fig. 7 ORTEP drawing of the molecular structure of **11g** (left) and **11f** (right). Thermal ellipsoids with 50% probability at 173 K (hydrogen atoms omitted for clarity). Selected distances (Å) and angles (°): **11g**: Bi1–N1 2.129(2), Bi1–N1′ 2.147(2), Bi1–N2 2.165(2), N1–Bi1–N2 95.29(8), N2–Bi1–N1′ 96.61(8), N1′–Bi1–N1 75.62(8), Bi1–N1–C1 127.0(2), C1–N1–Bi1′ 127.3(2), Bi1′–N1–Bi1 104.38(8), Bi1–N1–C1–C2 155.7(2); **11f**: Bi1–N1 2.16(1), Bi1–N2 2.164(7), Bi1–N3 2.176(9), N2–Bi2 2.154(9), Bi2–N1 2.142(7), Bi2–N4 2.175(9), N1–Bi1–N2 77.1(3), N2–Bi1–N3 99.5(3), N3–Bi1–N1 101.7(3), N1–Bi2–N2 77.7(3), N2–Bi2–N4 102.1(3), N4–Bi2–N1 98.7(3), Bi1–N2–C20 127.9(7), C20–N2–Bi2 129.7(6), Bi2–N2–Bi1 102.3(4), Bi1–N2–C20–C21 142.6(8).

(2.940–3.637 Å) which are well within the range of van der Waals radii ($\sum r_{\mathrm{vdW}}$(C···Bi) = 3.77 Å).[31]

Interestingly, this strong interaction led to a considerable distortion of the highly flexible terphenyl substituent as indicated by *e.g.* the deviation from planarity of the involved phenyl ring (largest C–C–C–C torsion angle 9.3°). In **5a** an intermolecular Menshutkin type π complex with one co-crystallized toluene solvent molecule is found with Bi···C$_{\mathrm{arene}}$ distances between 3.340–3.517 Å.

As depicted in Fig. 3 and 5, a chain-like structure arises for **5b** and **5e/9e** due to weak Cl···Bi interactions between adjacent molecules. In **5b** different Cl···Bi interactions can be discussed as indicated by the following four long range distances: Bi2′–Cl4 3.593(1), Bi2′–Cl2′ 3.359(1), Bi1′–Cl3′ 3.755(1), and Bi1–Cl3′ 3.761(1) Å. These rather long Bi···Cl distances (*cf.* $\sum r_{\mathrm{vdW}}$(Bi···Cl) = 3.81 Å)[31] are significantly longer than the intramolecular Bi–Cl bonds (2.449–2.506 Å, $\sum r_{\mathrm{cov}}$(Bi–Cl) = 2.50 Å)[29] in accord with a polar Bi–Cl single bond (see above).

To the best of our knowledge compound **5e/9e** is the first example of co-crystallized mono and double substituted aminochloropnictanes. Both species are linked by three Cl···Bi interactions (Bi1–Cl3 3.057(2), Bi2′–Cl1 3.516(2), and Bi2′–Cl2 3.644(2) Å, Fig. 5) leading to the formation one-dimensional chains along the *a*-axis with alternating **5e** and **9e** molecules in the solid state.

Conclusions

Depending on the steric demand of the aryl group and the used stoichiometry the reaction of RN(SiMe$_3$)Li with BiCl$_3$ leads to mono, double or even triple substitution at the bismuth atom. With bulky groups attached to the amide, preferentially the products of mono substitution (**5**) are found

(Scheme 3), while triple substitution is mainly observed for smaller groups. The aminodichlorobismuthanes **5** with smaller R groups readily undergo BiCl$_3$ elimination reactions to form diaminochlorobismuthanes (**9**) or even triaminobismuthanes (**12**). Instead of triaminobismuthanes also *cyclo*-dibismadiazanes **11** can be formed when an excess of amide with a less bulky group is used and in solution both compounds **11** and **12** can even co-exist as well as in the solid state. For bulky groups, which are not able to form triple substitution products, the reaction of a huge excess of amide with BiCl$_3$ leads to the formation of the amine RN(SiMe$_3$)H. We want to stress that all reaction conditions (stoichiometry, solvent, reaction temperature, the use of isolated lithium amide or *in situ* generated and use of sublimed or unsublimed BiCl$_3$) have a strong influence on the formed products and their distribution in mixtures. Even small changes to the reaction conditions can lead to very different results.

In the solid state the Lewis acidic bismuth atoms in these compounds can be stabilized by secondary interactions with aromatic solvents or intramolecularly, such as in the terphenyl substituted species. Another way to stabilize bismuth centers was established by bridging Cl atoms as found in some of the mono- and dichloro bismuthanes.

C–C coupling reactions rather than substitution was only observed for the supermesityl substituted derivative, which forms in the first step the mono-substitution product, that readily undergoes a C–C coupling process, presumably by a radical mechanism.

Acknowledgements

Notes and references

1 T. A. Hanna, A. L. Rieger, P. H. Rieger and X. Wang, *Inorg. Chem.*, 2002, **41**, 3590–3592.
2 I. J. Casely, J. W. Ziller, M. Fang, F. Furche and W. J. Evans, *J. Am. Chem. Soc.*, 2011, **133**, 5244–5247.
3 D. R. Kindra and W. J. Evans, *Dalton Trans.*, 2014, **43**, 3052–3054.
4 D. R. Kindra, I. J. Casely, J. W. Ziller and W. J. Evans, *Chem. – Eur. J.*, 2014, **20**, 15242–15247.
5 R. J. Schwamm, J. R. Harmer, M. Lein, C. M. Fitchett, S. Granville and M. P. Coles, *Angew. Chem., Int. Ed.*, 2015, **54**, 10630–10633.
6 H. Suzuki and Y. Matano, *Organobismuth Chemistry*, Elsevier Science B. V., Amsterdam, 2001.
7 G. He, O. Shynkaruk, M. W. Lui and E. Rivard, *Chem. Rev.*, 2014, **114**, 7815–7880.
8 (*a*) M. S. Balakrishna, D. J. Eisler and T. Chivers, *Chem. Soc. Rev.*, 2007, **36**, 650–664; (*b*) G. G. Briand, T. Chivers and M. Parvez, *Can. J. Chem.*, 2003, **81**, 169–174.

9 D. Michalik, A. Schulz and A. Villinger, *Angew. Chem., Int. Ed.*, 2010, **49**, 7575–7477.

10 M. Veith, B. Bertsch and V. Huch, *Z. Anorg. Allg. Chem.*, 1988, **559**, 73–88.

11 W. Baumann, A. Schulz and A. Villinger, *Angew. Chem., Int. Ed.*, 2008, **47**, 9530–9532.

12 M. Lehmann, A. Schulz and A. Villinger, *Angew. Chem., Int. Ed.*, 2012, **51**, 8087–8091.

13 R. J. Schwamm, B. M. Day, M. P. Coles and C. M. Fitchett, *Inorg. Chem.*, 2014, **53**, 3778–3787.

14 C. Hering-Junghans, M. Thomas, A. Villinger and A. Schulz, *Chem. – Eur. J.*, 2015, **21**, 6713–6717.

15 O. J. Scherer, P. Hornig and M. Schmidt, *J. Organomet. Chem.*, 1966, **6**, 259–264.

16 M. Veith and B. Bertsch, *Z. Anorg. Allg. Chem.*, 1988, **557**, 7–22.

17 A. J. Edwards, M. A. Beswick, J. R. Galsworthy, M. A. Paver, P. R. Raithby, M.-A. Rennie, C. A. Russell, K. L. Verhorevoort and D. S. Wright, *Inorg. Chim. Acta*, 1996, **248**, 9–14.

18 B. Nekoueishahraki, P. P. Samuel, H. W. Roesky, D. Stern, J. Matussek and D. Stalke, *Organometallics*, 2012, **31**, 6697–6703.

19 (*a*) B. M. Day and M. P. Coles, *Organometallics*, 2013, **32**, 4270–4278; (*b*) R. J. Schwamm, M. P. Coles and C. M. Fitchett, *Organometallics*, 2015, **34**, 2500–2507.

20 M. Brym, C. M. Forsyth, C. Jones, P. C. Junk, R. P. Rose, A. Stasch and D. R. Turner, *Dalton Trans.*, 2007, 3282–3288.

21 D. Dange, A. Davey, J. A. B. Abdalla, S. Aldridge and C. Jones, *Chem. Commun.*, 2015, **51**, 7128–7131.

22 B. N. Diel, T. L. Hubler and W. G. Ambacher, *Heteroat. Chem.*, 1999, **10**, 423–429.

23 W. Clegg, N. A. Compton, R. J. Errington, G. A. Fisher, M. E. Green, D. C. A. Hockless and N. C. Norman, *Inorg. Chem.*, 1991, **30**, 4680–4683.

24 N. Burford, T. S. Cameron, K.-C. Lam, D. J. LeBlanc, C. L. B. Macdonald, A. D. Phillips, A. L. Rheingold, L. Stark and D. Walsh, *Can. J. Chem.*, 2001, **79**, 342–348.

25 A. Schulz, *Z. Anorg. Allg. Chem.*, 2014, **640**, 2183–2192.

26 W. J. Evans, D. B. Rego and J. W. Ziller, *Inorg. Chim. Acta*, 2007, **360**, 1349–1353.

27 N. Burford, C. L. B. Macdonald, K. N. Robertson and T. S. Cameron, *Inorg. Chem.*, 1996, **35**, 4013–4016.

28 U. Wirringa, H. W. Roesky, M. Noltemeyer and H.-G. Schmidt, *Inorg. Chem.*, 1994, **33**, 4607–4608.

29 P. Pyykkö and M. Atsumi, *Chem. – Eur. J.*, 2009, **15**, 12770–12779.

30 H. Schmidbaur and A. Schier, *Organometallics*, 2008, **27**, 2361–2395.

31 M. Mantina, A. C. Chamberlin, R. Valero, C. J. Cramer and D. G. Truhlar, *J. Phys. Chem. A*, 2009, **113**, 5806–5812.